A remarkable caddisfly from the Vjosa River catchment: *Thremma anomalum* McLachlan 1876

Johann Waringer, Jan Martini & Simon Vitecek

This paper presents information on the morphology of the larval instars and the pupa of *Thremma anomalum* and illustrates the most important diagnostic features. In addition, we provide biometrical and ecological data with special reference to the Vjosa catchment.

Waringer J., Martini J. Vitecek S., 2020: Eine bemerkenswerte Köcherfliegenart aus dem Einzugsgebiet der Vjosa: *Thremma anomalum* McLachlan 1876:
Die vorliegende Arbeit beschreibt und illustriert die fünf Larvalstadien sowie die Puppe der Köcherfliege *Thremma anomalum* aus dem Einzugsgebiet der Vjosa. Ergänzt wird die Beschreibung durch biometrische und ökologische Daten.

Keywords: *Thremma anomalum,* Vjosa Rriver.

Introduction

Large riverscapes are complex ecosystems depending largely on hydrological dynamics. The lateral connectivity and exchange processes between the river and its floodplain are recognized as the most important feature of river-floodplain systems. During the last decades theoretical and applied limnological research more and more focused on the investigation of floodplain rivers (Amoros & Roux 1988; Junk et al. 1989; Henry & Amoros 1995; Sparks 1995; Ward & Stanford 1995; Schiemer 1999; Ward et al. 1999; Findlay et al. 2002; Gergel et al. 2002). Due to the pressures on riverine systems, such as regulation and damming, these spots of biodiversity have become one of the most threatened ecosystems (Dynesius & Nilsson 1994; Schiemer et al. 1999). The latter also fully applies to a wide range of rivers on the Balkan Peninsula, among them the Vjosa River in Greece and Albania which is one of Europe's last living and untamed wild rivers. The source of the Vjosa is near the Greek village of Vouvoussa; the first 80 kilometers of the headwaters are named Aoos which turns into Vjosa in Albania. The free-flowing course of the Vjosa has a length of over 270 kilometers and is composed of braided and meandering sections, gravel islands, backwater areas, steep valleys and floodplains up to two kilometers wide. However, what makes this river really outstanding internationally is the fact that almost all its tributaries are free-flowing and intact as well, creating a living rivers network that is without par in Europe (Graf et al. 2018; Anonymous 2019). In the framework of preliminary excursions aimed on exploring the macrozoobenthos inventory of the Vjosa, Graf et al. (2018) collected 91 taxa of Trichoptera, Plecoptera, Diptera, Megaloptera, Heteroptera, Coleoptera and Crustacea, mostly comprising typical elements of highly dynamic large rivers which have lost large areas of their former distribution in Europe. These riverine faunal elements are highly sensitive to changes of the natural hydromorphology. The species inventory was greatly expanded during follow-up excursions by Simon Vitecek and Jan Martini; the samples included, among others, all developmental stages of a very remarkable caddisfly species, *Thremma anomalum*. McLachlan 1876. Genus *Thremma* was established by McLachlan back in 1876 and consists of five European species and one European subspecies (Waringer et al. 2020). During the decades, the systematic position of genus *Thremma* changed frequently (Holzenthal et al. 2007). Nowadays, *Thremma*, together with the Holarctic genus *Neophylax* McLachlan 1871 (41 species) and the North American genus *Oligophlebodes* Ulmer 1905 (7 species) is again included in family Thremmatidae (Sheffield et al. 2019). In this paper we present information on the morphology of all larval instars and the pupa, and illustrate the most important diagnostic features. In addition, ecological characteristics and the distribution in the Vjosa are briefly discussed.

Fritz Schiemer has ever been heavily engaged in the conservation and protection of intact river-floodplain systems and in management procedures for improving their ecological conditions. Fritz is also fully aware and vigilant of the ecological situation on the Balkan peninsula where the biggest threat for rivers is hydropower: investors currently use the opportunity to engage in a virtual construction boom of dams and power plants also in the valley of pristine rivers such as the Vjosa catchment. In order to honor his efforts in the protection and investigation of riverscapes we dedicate this paper to Fritz Schiemer on the occasion of his 80th birthday.

Methods

Sampling area

Thremma anomalum larvae and pupae were collected in a Vjosa tributary near Voidomatis (Greece), 30 m downstream of the Papingo Bridge (Site 40; 39°56'40.5"N, 20°41'15.8"E, 1245 m a.s.l.). The sampling site was situated over limestone bedrock, and consisted largely of mesolithal (6.3–20 cm, 55 %), macrolithal (20–63 cm, 15 %) and microlithal (2–6.3cm, 15 %), in minor fractions of megalithal (>63 cm, 5 %), akal (0.2–2 cm, 10 %) and psammal (<0.2cm, 5 %). A deciduous forest dominated the surrounding area. The handpicked larvae and pupae were collected in a riffle section of the stream on the backside of mesolithal sediment particles.

Adult specimens of *T. anomalum* were collected along riparian zones of the middle section of the Benca (Site 65; 40°14'57.4"N, 19°58'23.3"E). This tributary of the Vjosa is dominated by limestone bedrock, and is a sparsely vegetated area, with forest and minor fractions of agricultural land. The streambed consisted of mesolithal (65 %) and macrolithal (35 %), which were mostly overgrown by periphyton and filamentous algae.

Sampling methods

In order to characterize the aquatic invertebrate fauna of the Vjosa, sampling sites were distributed over the entire catchment. Larvae and pupae were sampled according to the multi-habitat sampling procedure using a 25 × 25 cm net (500µm mesh size; AQEM Con-

Plate 1: *Thremma anomalum*, fifth instar larva. Fig. 1: Head, frontolateral (a = antenna; op = occipital patch). Fig. 2: Head, ventral (va = ventral apotome; ps = pennate seta). Fig. 3: Left mandible, ventral (a = apex; c = central section; e = median straight edge; s = concave edge). Fig. 4: Thorax, dorsal (am = anteromedian sclerite; ams = anteromedian seta; l = lateral sclerite; ms = mesonotum; mt = metanotum; p = pronotal sclerite; pm = posteromedian sclerite; Fig. 5: Prosternum, ventral (ae = anterior extension; pe = posterior extension; ph = prosternal horn). Scale bars: 0,5 mm (except Fig. 3: 0,2 mm). – Tafel 1: *Thremma anomalum*, fünftes Larvenstadium. Fig. 1: Kopf, frontolateral (a = Antenne; op = Occipitalfleck). Fig. 2: Kopf, ventral (va = Submentum; ps = Fiederborste). Fig. 3: Linke mandibel, ventral (a = Apex; c = Mandibelkörper; e = mediane gerade Schneide; s = konkave Schneide). Fig. 4: Thorax, dorsal (am = anteromedianes Sklerit; ams = anteromediane Borsten; l = laterales Sklerit; ms = Mesonotum; mt = Metanotum; p = Pronotum; pm = posteromedianes Sklerit; Fig. 5: Prosternum, ventral (ae = vordere Verbreiterung; pe = hintere Verbreiterung; ph = Prosternalhorn). Maßstab: 0,5 mm (außer Fig. 3: 0,2 mm).

sortium 2002). The specimens were preserved in 4% Formaldehyde. Additional larval, pupa and adult specimens were collected by handpicking or by using hand nets. Adult specimens of *T. anomalum* were collected with sweeping nets. These specimens were preserved in 96% EtOH. Specimens were identified and photographed with a Nikon SMZ 1500 binocular microscope.

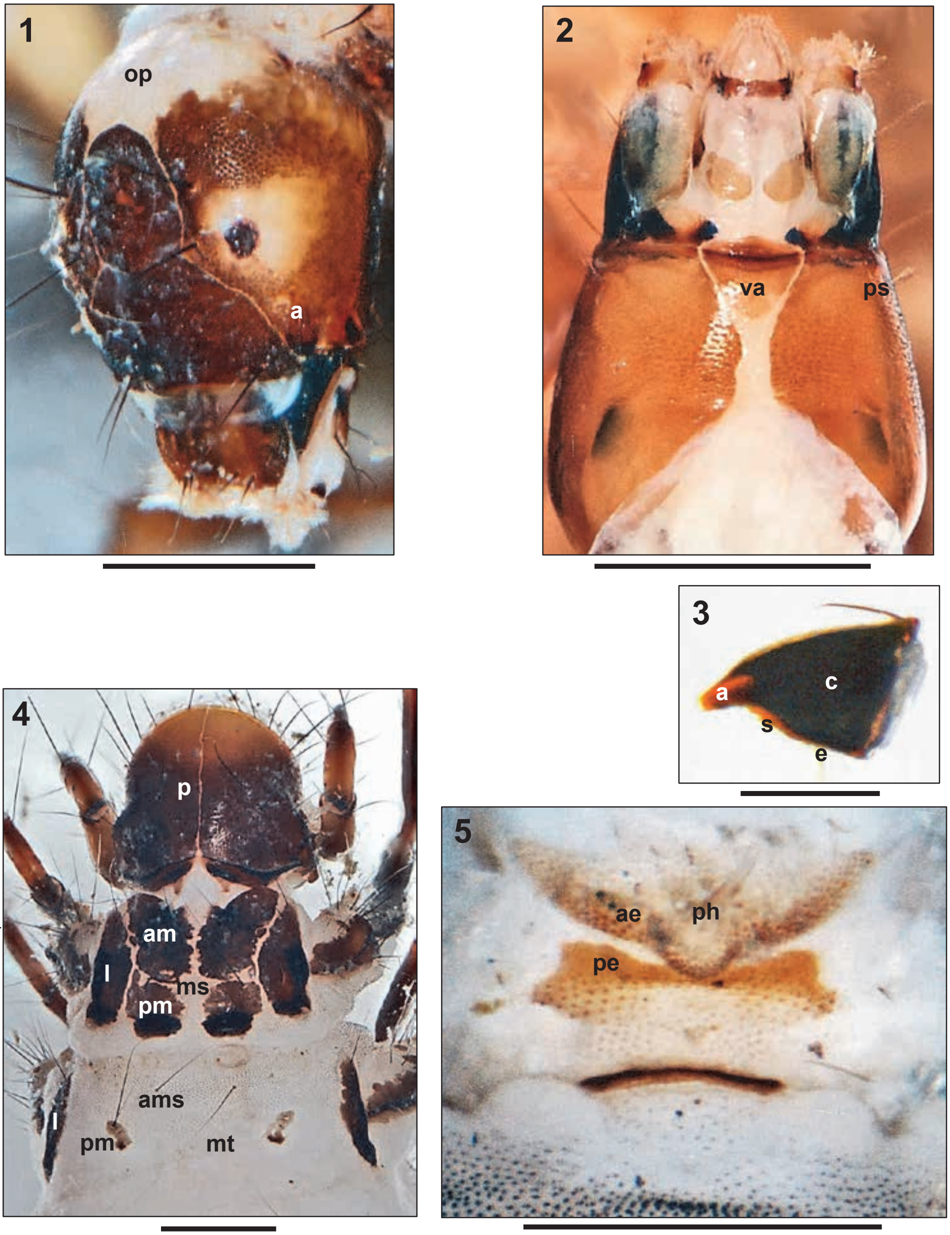

Biometry

In biometric studies, when plotting instar number against head width of the larvae, a straight line on a semilogarithmic scale indicates that the relationship between head width (y; mm) and instar number (x) is exponential and given by the regression equation $\ln y = \ln a + bx$, where a and b are constants. In case of a good data fit, the average head width increment per moult is proportionately constant, and Dyar's rule is applicable.

Results

Description of final (fifth) instar larva

The larva has been described by Stanković (1928), Botosaneanu (1956), and, more recently, redescribed by Waringer et al. (2020). We add details to those descriptions with special reference to early instars.

Body length 4,9–6,0 mm, head width 0,64–0,76 mm (n = 7). Head capsule slightly elongated, hypognathous, medium to dark brown, with distinct granulation most obvious in posterior section of frontoclypeal apotome. With whitish patches posterior of each eye (Fig. 1). White occipital patch (Fig. 1 op) without muscle attachment spots, strongly extending laterally when approaching occiput. Frontoclypeal apotome bell-shaped, with deep central constriction at eye level (Fig. 1). All primary setae simple except one pair of pennate setae (Fig. 2 ps). Antennae short and inconspicuous, originating from socket-like base halfway between eyes and anterior end of parietalia (Fig. 1 a). Posterior two thirds of ventral apotome yellowish brown, anterior third dark brown (Fig. 2 va). Labrum quadrangular, medium brown, with darker anterolateral patches, corners rounded. Anterolateral labral border membraneous, creating two white pads with numerous short setae (Fig. 1). Mandibles symmetrical, with black central section (Fig. 3 c) and straight median edges (Fig. 3 e) and apex; terminal scraper cutting edge lacking terminal teeth, extending from narrow ventral apex (Fig. 3 a) over tip of mandible to enlarged dorsal, semicircular edge (Fig. 3 s).

Brown pronotum consisting of two plates meeting in straight, narrow ecdysial suture (Fig. 4 p). Posterior pronotal half distinctly wider than anterior half, creating a shallow lateral constriction (Fig. 4). Anterior border with dense fringe of short, curved, fine, yellow setae; in addition, 20–24 setae of varying lengths distributed over each pronotal half (Fig. 4). Mesonotum (Fig. 4 ms) incompletely covered by 3 pairs of large sclerites: anteromedian sclerites wing-shaped, brown, with smooth, gently curving, convex median outline (Fig. 4 am). Posteromedian mesonotal sclerites (Fig. 4 pm) trapezoidal, posterolateral scle-

Plate 2: *Thremma anomalum*, fifth instar larva. Fig. 6: right foreleg, posterior face (pp = propleuron; t = foretrochantin). Fig. 7: right midleg, posterior face. Fig. 8: right hind leg, posterior face. Fig. 9: Detail of left lateral protuberance (sa = spinule area). Fig. 10: ventral protuberance of abdominal segment I, ventral (m = row of muscle attachment spots; sa = posterior spinule area; vs = ventral sclerite). Fig. 11: tip of abdomen, dorsal. Scale bars: 0,5 mm. – Tafel 2: *Thremma anomalum*, fünftes Larvenstadium. Fig. 6: rechtes Vorderbein, Hinteransicht (pp = Propleuron; t = Trochantinus). Fig. 7: rechtes Mittelbein, Hinteransicht. Fig. 8: rechtes Hinterbein, Hinteransicht. Fig. 9: linke laterale Protuberanz (sa = Spinulae). Fig. 10: ventrale Protuberanz des ersten Abdominalsegments, Ventralansicht (m = Reihe von Muskelansatzmarken; sa = Spinulae; vs = ventrales Sklerit). Fig. 11: Abdomenspitze von dorsal. Maßstab: 0,5 mm.

rites (Fig. 4l) broadly lenticular. Sometimes, anterolateral corner of posteromedian sclerite separated, thereby creating 1 or 2 tiny additional sclerites on mesonotum. Metanotum largely unsclerotized (Fig. 4 mt), with one pair of anteromedian setae (Fig. 4 ams), one pair of tiny posteromedian sclerites with 3 setae each (Fig. 4 pm), and one pair of elongate lateral sclerites (Fig. 4 l). Prosternum with anterolateral (Fig. 5 ae) and posterolateral extensions covered by spinule areas (Fig. 5 pe); prosternal horn present (Fig. 5 ph).

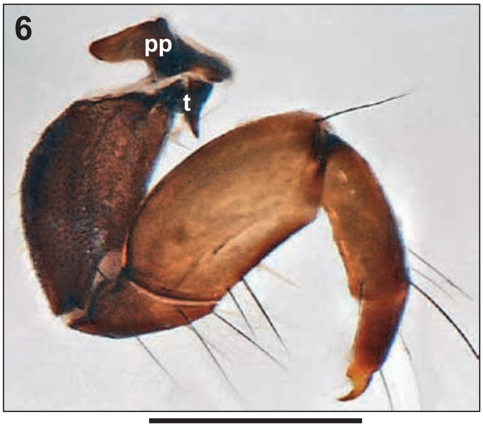

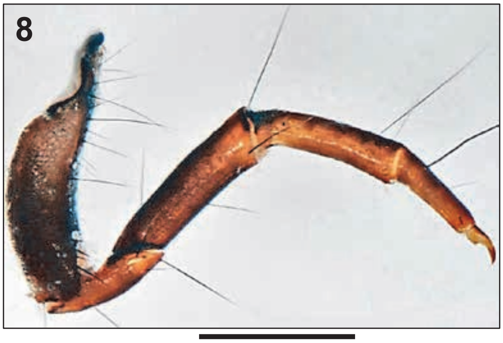

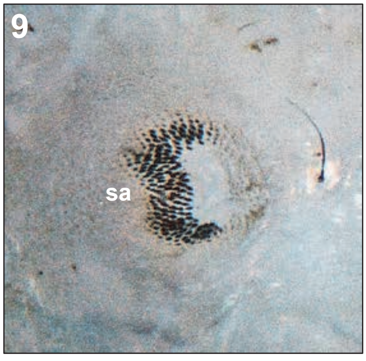

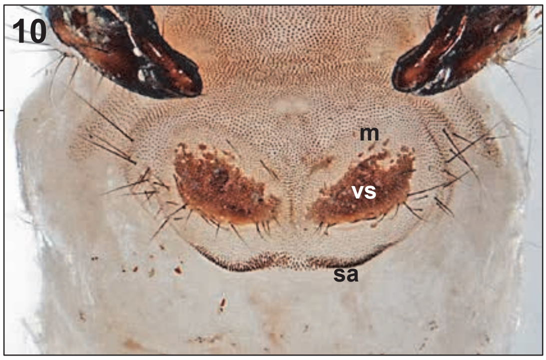

Legs brown with numerous setae on coxae, trochanters, and femora; tibiae and tarsi with only small number of setae (Fig. 6–8). Coxa, femur, and tibia of each foreleg much wider than those of mid- and hind legs; forefemur ratio (= maximum length divided by maximum width) is > 2 (Fig. 6). Propleuron (Fig. 6 pp) in close contact with ventral border of pronotum; with long, straight, pointed foretrochantin (Fig. 6 t); claw hook-shaped, with stout base bearing short pale seta (Fig. 6). Claw bases of mid- and hind legs much narrower than in forelegs; claws longer and sickle-shaped (Figs. 7, 8). Face setae lacking on femora of all legs.

Abdomen stout, almost cuneiform, with widths of abdominal segments gradually diminishing posteriorly. First abdominal segment with one dorsal, one ventral and one pair of lateral fleshy protuberances (Figs. 10, 14). Lateral protuberance with semicircular spinule area pointing in anterior direction (Fig. 9 sa). Pair of sclerites on ventral protuberance of abdominal segment I semicircular, brown, with narrow posterior and roundish anterior section (Fig. 10 vs), the latter with semicircular row of muscle attachment spots along median border (Fig. 10 m). Median borders of sclerites defining V-shaped soft cuticulous area. Sclerites and surrounding soft cuticle densely covered by spinules and 58–68 setae of various length, including setal rows along posterior borders of ventral sclerites (Fig. 10). With setal area along posterior border of ventral protuberance (Fig. 10 sa). Tergite IX brown, trapezoidal, with 12–14 setae of varying length along its posterior border (Figs. 11, 12 t). With mono- to trifilament gills. Dorsal and ventral gills present at most from abdominal segment II (postsegmental position) to segment VI (postsegmental position).

Case made of mineral particles, dorsoventrally flattened, strongly tapering, with anterior opening situated ventrally, without lateral wings, 4,9–6,2 mm long, maximum width at end of anterior third 2,2–2,8 mm, minimum width at posterior end 0,8–1,1 mm (Fig. 13). Posterior case opening partly closed by brown silken membrane; foramen posterior narrow and ovoid, near dorsal border of membrane and in transverse position.

Description of earlier instar larvae

Head width data for the five larval instars of *Thremma anomalum* (Fig. 14) are given in Table 1, and the most important discrimination characters valid also for instars 1 to 4 are summarized in Table 2. Sclerotization patterns of thoracic nota and on ventral protuberance on abdominal segment I are in line with the situation of final instars (Fig. 15–23). However, the white occipital patch which is very prominent in final instar larvae (Fig. 1 op) gradually becomes indistinct in earlier instars (e.g., Fig. 22).

Plate 3: *Thremma anomalum*, larva. Fig. 12: Fifth instar larva, tip of abdomen, right lateral (ac = anal claw; ls = lateral sclerite; t = tergite of abdominal segment IX). Fig. 13: Larval cases, ventral, of fifth instar (left) and third instar larva (right). Fig. 14: First to fifth instar larvae, dorsal. Fig. 15: First instar, head and thorax, dorsal. Fig. 16: First instar, head and thorax, ventral. Scale bars: 0,5 mm (except Figs. 15, 16: 0,2 mm). – Tafel 3: *Thremma anomalum*, Larve. Fig. 12: Fünftes Larvenstadium, Abdomenspitze von rechts lateral (ac = Analkralle; ls = Lateralsklerit; t = Tergit des neunten Abdominalsegments). Fig. 13: Larvenköcher von ventral, links fünftes, rechts drittes Stadium. Fig. 14: erstes bis fünftes Larvenstadium, Dorsalansicht. Fig. 15: erstes Larvenstadium, Kopf und Thorax von dorsal. Fig. 16: erstes Larvenstadium, Kopf und Thorax von ventral. Maßstab: 0,5 mm (außer Fig. 15, 16: 0,2 mm).

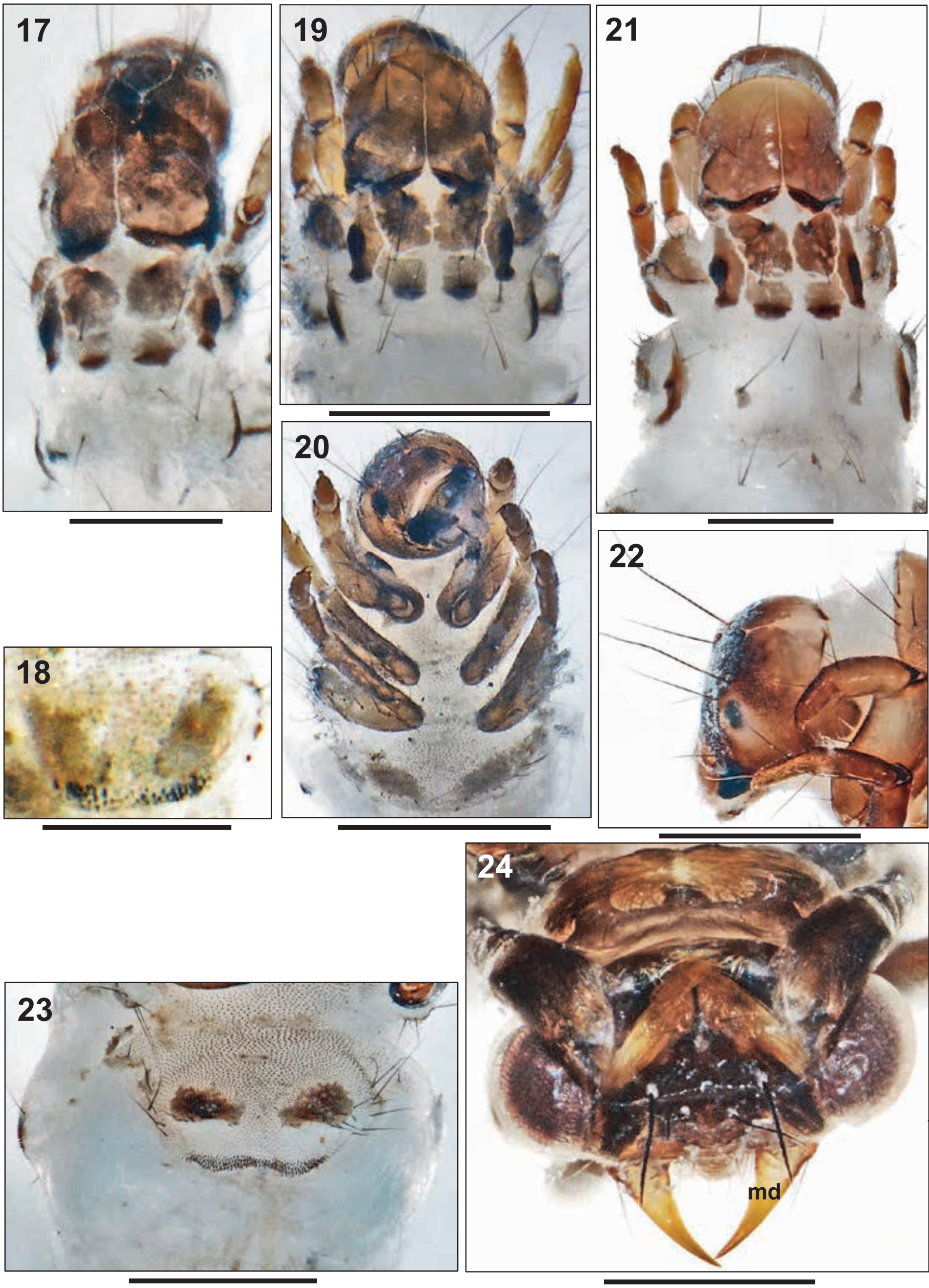
17
19
21
20
18
22
24
23
md

Tab. 1: Head width data for the larval instars of *Thremma anomalum*. – Tab. 1: Kopfkapselbreiten der Larvenstadien von *Thremma anomalum*.

Instar	Head width (range; mm)
1	0,16
2	0,21 – 0,22
3	0,30 – 0,35
4	0,46 – 0,53
5	0,64 – 0,76

Biometry of larvae

At our site, all larval instars were present at the collection dates. A frequency distribution histogram of head widths of the larvae (Fig. 29 a) clearly separates the larvae into instars 1–5; head width data of the five larval instars are summarized in Table 1. The semilog equation was a good fit to the data, and F-values from the variance ratio were

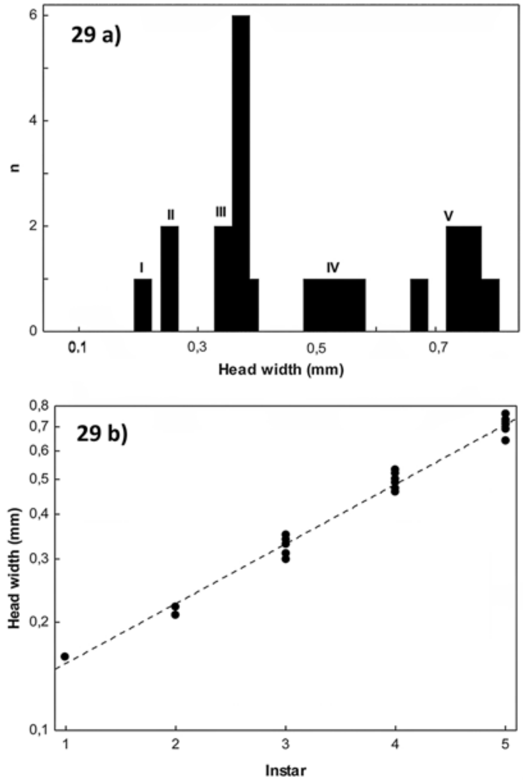

Fig. 29a: Size-frequency plot of head width data of 25 larvae of *Thremma anomalum*. The five instars are marked by roman numerals. Fig. 29b: Semilog relationship between instar number and head width of 25 larvae of *T. anomalum*. The regression was very highly significant ($P< 0.001$; $r^2 = 0{,}99$) and given by: $\ln y = -2{,}26 + 0{,}38x$. – Fig. 29a: Kopfkapselbreitenverteilung der fünf Larvalstadien von *Thremma anomalum* (n = 25). Die Larvalstadien sind mit römischen Ziffern markiert. Fig. 29b: Semilogarithmische Beziehung zwischen Larvalstadium und Kopfkapselbreite von 25 Larven von *T. anomalum*. Die Regression war hoch signifikant ($P< 0.001$; $r^2 = 0{,}99$); die Regressionsgleichung lautet: $\ln y = -2{,}26 + 0{,}38x$.

Plate 4: *Thremma anomalum*. Fig. 17: Second instar, head and thorax, dorsal. Fig. 18: Second instar, ventral protuberance on abdominal segment I, ventral. Fig. 19: Third instar, head and thorax, dorsal. Fig. 20: Third instar, head, thorax and abdominal segment I, ventral. Fig. 21: Fourth instar, head and thorax, dorsal. Fig. 22: Fourth instar, head, left dorsolateral. Fig. 23: Fourth instar, ventral protuberance on abdominal segment I, ventral. Fig. 24: Pupa, head dorsal (md = mandible). Scale bars: 0,5 mm (except Figs. 17, 18: 0,2 mm). – Tafel 4: *Thremma anomalum*. Fig. 17: zweites Larvenstadium, Kopf und Thorax von dorsal. Fig. 18: zweites Larvenstadium, ventrale Protuberanz am ersten Abdominalsegment, ventral. Fig. 19: drittes Larvenstadium, Kopf und Thorax von dorsal. Fig. 20: drittes Larvenstadium, Kopf, Thorax und erstes Abdominalsegment, ventral. Fig. 21: viertes Larvenstadium, Kopf und Thorax, dorsal. Fig. 22: viertes Larvenstadium, Kopf, dorsolateral. Fig. 23: viertes Larvenstadium, ventrale Protuberanz am ersten Abdominalsegment, ventral. Fig. 24: Puppe, Kopf dorsal (md = Mandibel). Maßstab: 0,5 mm (außer Fig. 17, 18: 0,2 mm).

Tab. 2: Morphomatrix defining the larvae of *Thremma anomalum*. – Tab. 2: Morphologische Schlüsselmerkmale für die Larven von *Thremma anomalum*.

Pronotum completely, mesonota and metanota incompletely sclerotized (Figs. 4, 15, 17, 19, 21);
Mesonotum covered by 3 pairs of large sclerites in typical arrangement (Figs. 4, 15, 17, 19, 21);
Prosternal horn present (Fig. 5 ph);
First abdominal segment with one dorsal, one ventral and one pair of lateral fleshy protuberances (Figs. 10, 14);
Ventral protuberance with pair of sclerites (Figs. 10, 16, 18, 20, 23);
Case made of mineral particles, dorsoventrally flattened, strongly tapering, with anterior opening situated ventrally (Fig. 13).

very highly significant (P<0.00l). The proportion (r^2) of the variance of y due to the regression of y on instar number was 0.99 (Fig. 29 b). Therefore, Dyar's rule was applicable.

Description of pupa

Head width 1,2 mm, body length 5,5 mm. Labrum with fine wrinkles, convex, with unhooked setae (Fig. 24). Antennae slightly longer than body, not coiled around tip of abdomen (Fig. 25). Mandibles symmetrical, each with only a single apical tooth, without mesal serrations (Fig. 24 md). Abdominal segments I and II without hook plates; one pair of anterior (Fig. 27 a) and one pair of posterior hook plates on abdominal segment V (Fig. 27 p), remaining abdominal segments with one pair of hook anterior plates each (Fig. 26, 28). Lateral fringe present on abdominal segments V–VIII (Fig. 25 lf). Abdomen terminated in a pair of slender, sclerotized anal processes crossed over one another, with only few setae (Fig. 28 ap). Pupal case mineral, tubular, strongly tapering posteriorly and dorsoventrally slightly flattened, with anterior opening situated ventrally. A morphomatrix defining the pupa of *Thremma anomalum* is given in Table 3.

Tab. 3: Morphomatrix defining the pupa of *Thremma anomalum* (partly after Wiggins & Currie 2008). – Tab. 3: Morphologische Schlüsselmerkmale der Puppe von *Thremma anomalum* (teilweise nach Wiggins & Currie 2008).

Each mandible with only a single apical tooth, without mesal serrations (Fig. 24);
Labrum with straight, unhooked setae (Fig. 24);
Antenna little longer than body, not coiled around tip of abdomen (Fig. 25);
Abdominal segments with dorsal setae single, not arranged in clusters (Fig. 26);
Abdominal segments I and II without hook plates; two pairs of hook plates on abdominal segment V, remaining abdominal segments with one pair of hook plates each (Fig. 26);
Abdomen with lateral fringe continuous from segment V to VIII (Fig. 25 lf);
Abdomen terminated in a pair of slender, sclerotized anal processes crossed over one another, with only few setae (Fig. 28 ap);
Pupal case mineral, tubular, strongly tapering posteriorly and dorsoventrally slightly flattened, with anterior opening situated ventrally.

Plate 5: *Thremma anomalum*, pupa. Fig. 25: pupa, left lateral (lf = lateral fringe). Fig. 26: abdominal segments I to V, dorsal. Fig. 27: detail of abdominal segment V, dorsal (a = anterior hook plate; p = posterior hook plate). Fig. 28: abdominal segments V to X, dorsal (ap = anal processes). Scale bars: 0,5 mm. – Tafel 5: *Thremma anomalum*, Puppe. Fig. 25: Puppe, lateral (lf = Seitenlinie). Fig. 26: erstes bis fünftes Abdominalsegment, dorsal. Fig. 27: fünftes Abdominalsegment, dorsal (a = vordere Häkchenplatte; p = hintere Häkchenplatte). Fig. 28: fünftes bis zehntes Abdominalsegment, dorsal (ap = Analfortsatz). Maßstab: 0,5 mm.


25
lf

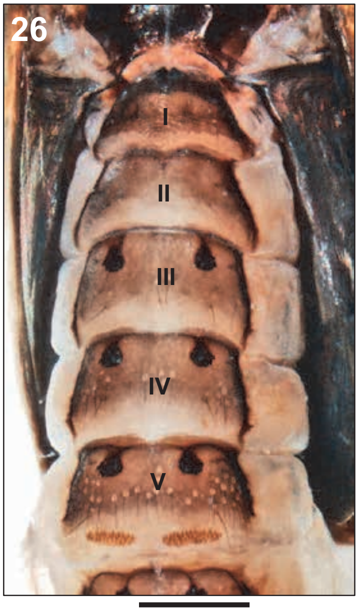
26
I
II
III
IV
V

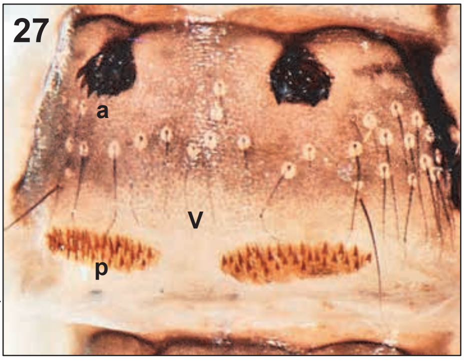
27
a
V
p

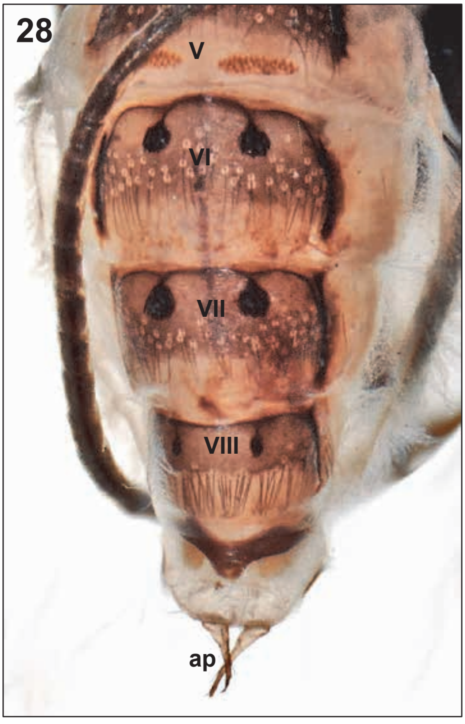
28
V
VI
VII
VIII
ap

Ecology and distribution

For *Thremma* species, ecological information is rather scarce. During his collection trips throughout Europe, Malicky collected large series of water temperature data (Malicky 2014) allowing an insight into typical thermal requirements for the European species inventory. Observed spring to autumn water temperatures in streams frequented by *Thremma anomalum* in Greece (Vermion mountains at Imatias, 1450 m a.s.l.; Agios Paraskevi, 1100 m a.s.l.; Rhodope mountains at Elatias, 1450 m a.s.l.; Vlachovuni mountains near Pendayi, 900 m a.s.l.; Peloponnese at Taygetos, 1000 m a.s.l.; Euboea near Stropones, 700–950 m a.s.l.) ranged from 5.2 to 16.8° C. A unique feature in genus *Thremma* are the special cases which are hypothesized to minimize hydraulic stress and also protect against predators, since the cases attach closely to the substrate (Wichard et al. 1995, Kehl 2005). In some species (e.g., *T. gallicum* and *T. sardoum*), cases consist of a central tube and lateral wing-like extensions with irregular borders; however, this is not the case in *T. anomalum* (Fig. 13).

The mandibles with their smooth cutting edges which lack terminal teeth (Fig. 3) signify that *Thremma* species feed mainly in a scraper role by grazing on fine particulate organic matter and Bacillariophyceae attached to mineral sediment particles. These assumptions were corroborated by observations and gut analyses conducted by Jacquemart & Coineau (1966), Giudicelli (1971) and González et al. 1989a. With respect to phenology, the 80 adult specimens of *T. anomalum* included in the Zobodat database (Zobodat 2019) were sampled between 18 April and 23 October. As virtually all developmental stages were collected in the Vjosa catchment simultaneously, the life cycle seems to be badly synchronized. This is also the case in other *Thremma* species, e.g., *T. tellae*, where adults are on the wing practically all year round from January to November (González 1988; González et al. 1989b).

The distribution range of *T. anomalum* is one of the largest of all European *Thremma* species, covering six ecoregions (Graf et al. 2008; Neu et al. 2018). The species has been recorded on the Dinaric Western, Hellenic Western and Eastern Balkan, the Carpathians, Pontic Province, and Caucasus area. In terms of national borders, the species is known from Albania, Bosnia and Herzegowina, Bulgaria, the Greek Mainland, Northern Macedonia, Romania, Serbia, and Turkey. Recent investigations modified the western boundary of *T. anomalum*: while the species is declining in western Serbia, northern Montenegro and Bosnia and Herzegovina, *T. anomalum* was found at 17 localities in eastern, southeastern and southern Serbia where the species was not recorded before (Živić et al. 2013).

Acknowledgments

Fieldwork in the Vjosë catchment was conducted with support from the FLUFLUX project (Fluvial Meta-Ecosystem Functioning: Unravelling Regional Ecological Controls Behind Fluvial Carbon Fluxes) funded by the European Research Council (ERC-STG 716196).

Literature

Amoros C. & Roux A.L., 1988: Interaction between water bodies within the floodplains of large rivers: function and development of connectivity. Münstersche Geograph. Arbeiten 29, 125–130.

Anonymous, 2019: Save the Blue Heart of Europe. Available from: https://www.balkanrivers.net/en/key-areas/vjosa-river (accessed 19 June 2019).

AQEM Consortium, 2002: Manual for the application of the AQEM system. Developed and written by the AQEM consortium, 1–202.

Botosaneanu L., 1956: Recherches sur les trichoptères de Bulgarie recueillis par MM. le Prof. Valkanov et B. Rusev. Beitr. zur Entomologie 6, 354–402.

Dynesius M. & Nilsson C., 1994: Fragmentation and flow regulation of river systems in the northern third of the world. Science 266, 753–762.

Findlay E.G., Kiviat E., Nieder W.C. & Blair E.A., 2002: Functional assessment of a reference wetland set as a tool for science, management and restoration. Aquatic Sciences 64, 107–117.

Gergel S.E., Turner M.G., Miller J.R., Melack J.M. & Stanley E.H., 2002: Landscape indicators of human impacts to riverine systems. Aquatic Sciences 64, 118–128.

Giudicelli J., 1971: Monographie du genre *Thremma*. Trichoptera, Thremmatidae. Ann. Limnol. 7, 125–139.

González M.A., 1988: Inventario dos Tricópteros de Galicia (Insecta: Trichoptera). Cadernos Área Ciencias Biolóxicas: Inventarios. Seminario de Estudos Galegos, vol. II. Ediciós do Castro, 45 pp.

González M.A., Iglesias J.C. & Cobo F., 1989a: Description de la larve et considerations sur l'habitat, la biologie et la répartition de *Thremma tellae* (Trichoptera: Uenoidae: Thremmatinae). Ann. Limnol. 25, 237–241.

González M.A., Valiela J. & Cobo F., 1989b: Observaciones sobre los Tricópteros de la Península Ibérica. VIII: Sierras de Ancares y del Caurel (Noroeste de España) (Trichoptera). Boletín Asociación española de Entomología 13, 331–341.

Graf W., Murphy J., Dahl J., Zamora-Muñoz C. & López-Rodríguez M.J., 2008: Volume 1 – Trichoptera. In: Schmidt-Kloiber A. & Hering D. (eds.), Distribution and Ecological Preferences of European Freshwater Organisms. Pensoft Publishers, Sofia, Moscow.

Graf W., Grabowski M., Hess M., Heckes U., Rabitsch W. & Vitecek S., 2018: Contribution to the knowledge of aquatic invertebrate Fauna of the Vjosa in Albania. Acta ZooBot Austria, 155,135–153.

Henry C.P. & Amoros C., 1995: Restoration ecology of riverine wetlands: I. A scientific base. Environm. Management 19, 891–902.

Holzenthal R.W., Blahnik R.J., Prather A.L. & Kjer K.M., 2007: Order Trichoptera Kirby, 1813 (Insecta), Caddisflies. Zootaxa 1668, 639–698.

Jacquemart S. & Coineau Y., 1966: A propos de *Thremma gallicum* Mac Lachlan. Bulletin de l'Institut Royal des Sciences Naturelles Belgique, 42, 1–14.

Junk W.J., Bayley P.B. & Sparks R.E., 1989: The flood pulse concept in river floodplain systems. Canad. J. Fisheries and Aquat. Sci. 106, 110–127.

Kehl S., 2005: *Thremma gallicum* McLachlan, 1880: Zur Biologie, Ökologie und Verbreitung einer faunistischen Besonderheit Deutschlands. Entomologie heute, 17, 13–26.

Malicky H., 2014: Lebensräume von Köcherfliegen (Trichoptera). Denisia, 34, 1–280.

Neu P.J., Malicky H., Graf W. & Schmidt-Kloiber A., 2018: Distribution Atlas of European Trichoptera. Die Tierwelt Deutschlands, vol. 84. Goecke & Evers, Keltern.

Schiemer F., 1999: Conservation of biodiversity in floodplain rivers. Arch. Hydrobiol. Suppl. 115 (Large Rivers 11), 423–438.

Schiemer F., Baumgartner C. & Tockner K., 1999: Restoration of floodplain rivers: the Danube restoration project. Regulated Rivers: Research & Management 15, 23 1–244.

Sheffield C.S., deWaard J.R., Morse J.C. & Rasmussen A.K., 2019: Trichoptera of Canada. ZooKeys 819, 507–520.

Sparks R.E., 1995: Need for ecosystem management of large rivers and their floodplains. BioScience 45, 168–182.

Stanković S., 1928: On a new larva and nymph of Trichoptera, *Thremma* sp. Glasnik Skopskog Naučnog Društva. Odeljenje Prirodnih Nauka (Bulletin de la Société Scientifique de Skoplje. Section des Sciences Naturelles) 4, 121–128.

Ward J.V. & Stanford J.A., 1995: Ecological connectivity in alluvial river ecosystems and its disruption by flow regulation. Regulated Rivers: Research & Management 11, 105–119.

Ward J.V., Tockner K. & Schiemer F., 1999: Biodiversity of floodplain river ecosystems: ecotones and connectivity. Regulated Rivers: Research & Management 15, 125–1 39.

Waringer J., Gonzalez M. & Malicky H., 2020: Discriminatory matrix for the larvae of the European *Thremma* species (Trichoptera: Thremmatidae). Zootaxa 4718, 451–469.

Wichard W., Arens W. & Eisenbeis G., 1995: Atlas zur Biologie der Wasserinsekten. Gustav Fischer, Stuttgart, Jena, New York.

Wiggins G.B. & Currie D.C., 2008: Trichoptera families. In Merritt R.W., Cummins K.W. & Berg M.B. (eds.): An introduction to the aquatic insects of North America, 439–480. 4th edition. Kendall/Hunt, Dubuque, Iowa.

Živić I., Bjelanović K., Simić V., Živić M., Žikić V. & Marković Z., 2013: New records of *Thremma anomalum* (Trichoptera: Uenoidae) from southeastern Europe with notes on its ecology. Entomological News, 206–219.

Zobodat, 2019: Zoological-Botanical Database of the State Museum of Upper Austria. Available from: http://www.biologiezentrum.at/de/bz/ (accessed 13 May 2019).

Received: 2020 01 28

Addresses:

Univ.-Prof. Dr. Johann Waringer, E-Mail: johann.waringer@univie.ac.at
Jan Martini, MSc., E-Mail: elvanjan@gmail.com
Division Limnology, Department of Functional and Evolutionary Ecology, University of Vienna, Althanstrasse 14, A-1090 Vienna, Austria.

Dr. Simon Vitecek, WasserCluster Lunz, Dr. Carl Kupelwieser Promenade 5, A-3293 Lunz am See, Austria. E-Mail: simon.vitecek@wkl.ac.at